Treatment of bone metastasis induced by MDA-MB-231 breast cancer cells with an antibody against bone sialoprotein

TOBIAS BÄUERLE[1], JENNY PETERSCHMITT[1], HEIDEGARD HILBIG[3], FABIAN KIESSLING[2], FRANZ P. ARMBRUSTER[4] and MARTIN R. BERGER[1]

[1]Unit of Toxicology and Chemotherapy, [2]Department of Medical Physics in Radiology, Deutsches Krebsforschungszentrum Heidelberg, Im Neuenheimer Feld 280, 69120 Heidelberg; [3]Institute of Anatomy, University of Leipzig, Liebigstr. 13, 04103 Leipzig; [4]Immundiagnostik AG, Wiesenstr. 4, 64625 Bensheim, Germany

Received October 18, 2005; Accepted November 25, 2005

Abstract. The extracellular bone matrix protein bone sialoprotein (BSP) is considered to play an important role in the pathogenesis of lytic skeletal lesions which are associated with severe morbidity in breast, prostate or lung cancer patients. In addition to *in vitro* studies, nude rats were implanted with 10^5 MDA-MB-231 cells transfected with GFP into a small branch of the femoral artery. Osteolytic lesions of the respective hind leg were detected by X-ray and CT analysis as well as by immunohistochemistry. Exposure of MDA-MB-231^{GFP} cells *in vitro* to an antibody against BSP (0-400 μg/ml) decreased proliferation, colony formation and migration of these cells by up to 95, 83 and 89 T/C%, respectively. In nude rats, preincubation of MDA-MB-231^{GFP} cells prior to inoculation (25-100 μg/ml) reduced the mean osteolytic lesion size to 22 T/C% after 90 days of observation ($p<0.05$). Treatment of overt lytic metastasis with the anti-BSP antibody (10 mg/kg) resulted in a significantly smaller mean lesion size of 57 T/C% at the end of the observation period ($p<0.05$) as well as in new bone formation. Immunohistochemical analysis revealed the presence of BSP in MDA-MB-231^{GFP} cells and in vessel endothelium cells during processes such as migration and invasion. In conclusion, an anti-BSP antibody decreased proliferation, colony formation and migration of MDA-MB-231^{GFP} cells *in vitro* and reduced osteolysis besides inducing bone formation in a nude rat model.

Correspondence to: Professor Martin R. Berger, Unit of Toxicology and Chemotherapy, Deutsches Krebsforschungszentrum Heidelberg, Im Neuenheimer Feld 280, D-69120 Heidelberg, Germany
E-mail: m.berger@dkfz.de

Abbreviations: anti-BSP, polyclonal chicken antibody against human BSP; BSP, bone sialoprotein; CT, computed tomography; GFP, enhanced green fluorescent protein; MDA-MB-231^{GFP}, MDA-MB-231 human breast cancer cells transfected with GFP; MMP, matrix metalloproteinase; SIBLING, small integrin-binding ligand N-linked glycoprotein

Key words: bone sialoprotein, anti-BSP antibody, MDA-MB-231 human breast cancer cell line, bone metastasis, nude rat model

Introduction

Metastases of several malignancies, including breast, prostate, lung, kidney and thyroid cancer, have high affinity for the skeleton. Bone metastasis is frequently paralleled by serious clinical complications such as pathologic fractures, spinal cord compression, bone pain and hypercalcaemia. In breast cancer, bone is the site of first distant relapse and the clinical course of these women is relatively long, with a median survival of 2-3 years (1,2). Skeletal metastases are present in over 90% of patients who die from breast cancer (3). In patients with primary breast cancer, elevated bone sialoprotein (BSP) serum levels were associated with presence of metastatic cells in lymph nodes and bone marrow, development of subsequent bone metastasis and poor prognosis in these patients (4-8). The expression of BSP has been demonstrated in primary breast cancer as well as in breast cancer bone metastasis (7,9-11).

BSP is a non-collagenous glycoprotein of the extracellular bone matrix and belongs to the SIBLING (small integrin-binding ligand N-linked glycoprotein) gene family. The SIBLINGs are clustered on human chromosome 4, and include bone sialoprotein (BSP), osteopontin (OPN), dentin matrix protein 1 (DMP1), matrix extracellular phosphoglycoprotein (MEPE) and dentin sialophosphoprotein (12). These proteins are normally expressed in mineralizing tissues of bone and teeth but are also found in different cancers (13). In normal bone, BSP is expressed by osteoblasts, osteoclasts and other skeleton-associated cell types, especially at sites of new mineral formation (12,14-16). In bone, BSP is a potential nucleator of hydroxyapatite formation and a specific marker of osteoblast differentiation (14). The sialoprotein is involved in hydroxyapatite and collagen binding, as well as in the attachment of bone cells including fibroblasts, osteoblasts and osteoclasts to solid surfaces (12,14,16-19).

Characteristic binding partners of BSP are the matrix metalloproteinase MMP-2 and the integrin α(v)ß3, which form a tri-molecular complex together with BSP and thereby increase the invasiveness of cancer cells (20).

Recently, we established a site-specific model of bone metastasis in nude rats, which is characterized by lytic lesions confined to the femur, tibia and fibula of a single hind leg (21). Using this model, we were able to show that down-regulation of BSP by antisense oligonucleotides as well as preventive treatment with an antibody against BSP decreases subsequent bone metastasis formation (21,22).

The purpose of our present study was to examine the role of BSP in the pathogenesis of breast cancer bone metastasis and to develop a targeted treatment against MDA-MB-231 human breast cancer cell mediated osteolysis.

To this aim, we investigated the effects of an antibody against BSP on proliferation, colony formation and migration of MDA-MB-231 human breast cancer cells *in vitro*. For assessing its effects *in vivo*, we treated nude rats with this antibody after inoculation of MDA-MB-231 cells as well as after the onset of lytic lesions.

Materials and methods

Cell lines and culture conditions. MDA-MB-231 human mammary carcinoma cells were obtained from the American Type Culture Collection (ATCC). A subline stably transfected with the enhanced GFP gene (pEGFP; Clontech) was kindly provided by Dr Danny R. Welch (Pennsylvania State University College of Medicine, Hershey, PA).

MDA-MB-231^{GFP} cells were kept as monolayer cultures in RPMI-1640 medium (Invitrogen, Karlsruhe, Germany) supplemented with 10% FCS (Sigma, Taufkirchen, Germany) and 2 mM L-glutamine under standard conditions (37˚C, humidified atmosphere, 5% CO_2). To all cultures of neomycin resistant MDA-MB-231^{GFP} cells 500 μg/ml Geneticin (G418; Invitrogen) was added. SAOS-2 human osteosarcoma cells were obtained from the DSMZ (No. 243) and cultivated as monolayer in McCoy's 5A medium containing 15% FCS and 2 mM L-glutamine. In order to keep the tumor cells in logarithmic growth, all cells were passaged 1-3 times per week depending on their growth rate.

In vitro assays

Proliferation assay. A volume of 100 μl RPMI medium per well containing 5x10^3 MDA-MB-231^{GFP} cells was plated onto 96-well plates (Microtest™, Becton-Dickinson, Heidelberg, Germany). After 24 h 100 μl medium was added containing the anti-BSP IgY antibody (Immundiagnostik, Bensheim, Germany) at final concentrations of 1-400 μg/ml anti-BSP antibody. The plates were kept under standard cell culture conditions for 1-7 days of incubation. Thereafter, 10 μl/well of 3-[4,5-dimethylthiazol-2-yl]-2,5-diphenyltetrazolium bromide (MTT; 10 mg/ml) was added to determine the number of surviving cells. The supernatant was removed after 3 h of incubation, and formazan crystals that had been developed were dissolved by adding of 100 μl acidified 2-propanol/well (0.04 N HCl). Extinction was measured by an automated microtiter plate reader at 540 nm, reference filter 690 nm (Anthos 2001, Anthos GmbH, Krefeld, Germany).

Colony formation assay. To determine the clonogenicity of MDA-MB-231^{GFP} cells after exposure to the anti-BSP IgY, 5x10^5 cells were pre-incubated for 48 h in 2 ml RPMI medium containing anti-BSP at concentrations of 1-400 μg/ml. Thereafter, MDA-MB-231^{GFP} cells were harvested, counted and transferred into semi-solid medium with 0.8% RPMI-methylcellulose and 30% FBS. Finally, 1 ml of the semi-solid medium containing 5x10^3 MDA-MB-231^{GFP} cells was plated onto 3.5 cm Petri-dishes (Nunc, Wiesbaden, Germany). Triplicate Petri-dishes per treatment protocol were cultivated for 5-7 days at standard cell culture conditions. Colony formation (clusters of ≥30 cells) was visualized by staining with MTT and scored by an inverted microscope.

Migration assay. In a model for cell migration (23), 1x10^3 MDA-MB-231^{GFP} cells were incubated with final anti-BSP IgY concentrations ranging from 1 to 200 μg/ml. They had been incubated for 48 h before being transferred into a transwell migration system. The breast cancer cells were plated on a polycarbonate filter membrane with a pore size of 8 μm (upper layer). The bottom layer was set up by 0.5 ml RPMI medium containing 1x10^4 SAOS-2 osteosarcoma cells, which were grown in 24-well plates (Nunc). After 24 h the medium was removed and a semi-liquid RPMI medium containing 0.2% methylcellulose and 20% FBS was transferred on top of the SAOS-2 cells (0.5 ml/well) in order to maintain a gradient between the two compartments and to provide an additional barrier for cell migration. The polycarbonate filter was removed from the bottom layer after 24 h of co-cultivation and transferred onto a fresh well containing bottom layer (see above). Cells migrating through the pores were counted daily for 4 days by fluorescence microscopy. The mean growth rate (MGR) of cells after migration through the polycarbonate filter was determined by the equation: $MGR = \log_2 N_t - \log_2 N_0/t$ (24), with N_0 as initial cell number, N_t as final cell number and t as time period of cell incubation in days.

Anti-bone sialoprotein immunoglobulin. Polyclonal antibodies developed in chicken against human bone sialoprotein were obtained from Immundiagnostik. Appropriate dilutions were made using PBS without Ca^{++} and Mg^{++}.

$ErPC_3$. The alkylphosphocholine erucylphospho-NNN-trimethylpropanolamine ($ErPC_3$) was synthesized and provided by Dr H. Eibl (MPI of Biophysical Chemistry, Göttingen, Germany). Appropriate dilutions were made using PBS without Ca^{++} and Mg^{++}.

Animals and husbandry. Nude rats (RNU strain) were obtained from Harlan Winkelmann (Borchen, Germany) and Charles River (Sulzfeld, Germany) at an age of 6-8 weeks. They were housed two per cage at specific pathogen-free conditions in a mini-barrier system of the central animal facility. Autoclaved feed and water was given *ad libitum* to the animals that were maintained under controlled conditions (21±2˚C room temperature, 60% humidity, and 12-h light-dark rhythm). Experiments were approved by the respective Animal Ethics Committee (Regierungspräsidium Karlsruhe, Germany).

In vivo metastasis model. Sub-confluent tumor cells were harvested using 2 mM EDTA in PBS$^-$ (phosphate-buffered saline without Ca^{++} and Mg^{++}) and 0.25% trypsin (Sigma). Cells were counted in a Neubauer's chamber and suspended in RPMI ($5x10^5$ cells/ml).

For tumor cell implantation, rats were anaesthetized with a mixture of laughing gas (nitrous oxide; 1 l/min), oxygen (0.5 l/min) and isoflurane (1-1.5 vol. %). A clear cut of 2-3 cm length was performed in the inguinal region. After preparation of the local arterial branching pattern descending from the femoral artery (FA), the blood flow was temporarily occluded by clips (21). The superficial epigastric artery (SEA), which branches off the FA, was ligated distally. A ligation of the distal SEA is possible because it anastomoses with branches of the iliac artery. After making an incision proximal of the ligation, a needle was inserted into the SEA and 10^5 MDA-MB-231^{GFP} cells suspended in 0.2 ml medium were slowly injected. By using clips, the breast cancer cells were directed to the descending genicular and popliteal arteries, both supplying the knee joint and muscles of the leg.

Radiographic examination and computer tomography. Radiographic examinations of rats were made every 7-14 days under general anesthesia. The animals were fixed in a.p. and p.a. position on a Cronex 5 film (Agfa-Gevaert N.V., Mortsel, Belgium) and exposed to X-rays generated by a Vertix U at 40 kV and 1.4 mAs (Siemens, Erlangen, Germany). The X-ray films were processed by an automatic developing machine (Scopix LR 5200; Agfa, Köln, Germany) and the resulting images were scanned using a digital imaging program (Adobe Photoshop 6.0, Adobe Systems Inc.) with a resolution of 300 dpi. Analyses were done with a computer based imaging program (UTHSCSA Image Tool, University of San Antonio, TX) to measure the area of the lesion. Lesions of tibia and femur were ranked with regard to the respective extent; with circular defects being considered as most prone to fracture. Lesions of the fibula were excluded from this differentiation because of their limited size. High resolution computed tomography (HRCT) was performed using a multi-detector Somatom Plus 4 CT-scanner (Siemens). Whole animals were investigated with a native spiral scan (increment: 0.5 mm; kernel: 90) at 100 mAs and 120 kV. Based on CT slices with 0.5 mm thickness three-dimensional volume rendering reconstructions of the skeleton were performed using the Vitrea 2 workstation (Vital Images, Plymouth, MN).

Statistical analyses. For each group of animals, the mean total lesion size obtained from X-ray analysis was used to draw a curve of mean lesion size versus time after tumor cell inoculation. For statistical comparisons, the individual growth curves were interpolated and lesion sizes were computed for intervals of 10 days. For comparison between two groups, the one-sided Wilcoxon rank sum test was applied. p-values <0.05 were considered significant. Comparisons of parameters between groups, such as circular defects of cortical bone or soft tissue metastasis, were performed with the χ^2-test. p-values <0.05 were considered significant. For comparison of average daily growth rates between groups, the one-sided Wilcoxon rank sum test was applied. p-values <0.05 were considered significant.

Bone storage and histology. After storage in 70% ethanol, the specimens were embedded in Technovit 9100 New (Heraeus Kulzer, Wehrheim, Germany) according to the instructions for application. Thereafter, the embedded samples were mounted on blocks using Technovit 3040 (Heraeus Kulzer) in order to remove the samples from the embedding device. Before cutting a block into 5 μm thick sections (Supercut 2050, Reichert-Jung, Germany), it was wetted with 30% ethanol. The sections were removed and placed on pre-coated slides using 96% ethanol. Finally, the sections were covered with polyethylene foil, pressed at 37˚C overnight and then deplasticised before being stained.

For immuno-cytochemical staining, the sections were rinsed several times with 0.1 M phosphate-buffered saline (PBS, pH 7.4), incubated with 10% normal goat serum (Vector, Burlingham, USA) and diluted in PBS for 2 h. Thereafter, the sections were incubated with the primary antibodies against BSP (anti-human bone sialoprotein from Immundiagnostik AG, Bensheim, Germany: mouse monoclonal anti-human bone sialoprotein A 423.2, rabbit polyclonal anti-bone sialoprotein A 4218.1; monoclonal anti-rat bone sialoprotein from Jaro Sodek, Toronto, Canada), which were diluted 1:100 in PBS containing 2% bovine serum albumin (PBS-BSA).

After several rinses in PBS, sections were incubated for 2 h with a 1:200 dilution of secondary antibody goat anti-mouse-Cy3 (Jackson Immuno Research) in PBS-BSA. The preparations were rinsed again with PBS, counterstained using DAPI (Serva, Heidelberg, Germany), dried and cover slipped. Control sections were treated with non-specific mouse antibodies (IgG1, Dako), diluted and applied similarly to the specific antibody. Sections were studied fluorescence microscopically using a photomicroscope equipped with epifluorescence (Axiophot; Zeiss, Germany).

Subsequent sections were stained with hematoxylin and eosine (Merck Ag, Dietikon, Switzerland) for light microscopical features.

Results

In vitro study. In this part of the study, MDA-MB-231^{GFP} human breast cancer cells were exposed to an IgY antibody against bone sialoprotein in order to determine the effect on proliferation, colony formation and migration (Table I, Fig. 1).

Proliferation assay. Incubation of MDA-MB-231^{GFP} cells for up to 7 days with concentrations from 1 to 400 μg/ml anti-BSP antibody decreased the proliferation in a dose- and time-dependent manner as examined by MTT assay (Fig. 1A). The T/C% value of exposed cells decreased gradually from 101 (1 μg/ml) to 5 (400 μg/ml) after 7 days of incubation.

Colony formation assay. The same range of concentrations was chosen to study the colony formation of MDA-MB-231^{GFP} cells after exposure to the anti- BSP immunoglobulin (Fig. 2B). Following 2 days of pre-incubation in medium, colony formation on methyl cellulose was dose-dependently inhibited, with T/C% values ranging from 107 (1 μg/ml) to 17 (400 μg/ml).

Table I. Overview of *in vitro* results.

Assay	1 μg/ml	25 μg/ml	50 μg/ml	100 μg/ml	200 μg/ml	400 μg/ml
Proliferation assay[a]	100.9	86.9	77.1	62.7	26.9	5.3
Colony formation assay[b]	106.6	94.2	86.4	54.2	43.2	17.3
Migration assay[c] (MGR)[d]	145.5 (0.72)	91.5 (0.64)	86.6 (0.69)	31.3 (0.32)	10.7 (0.25)	-

[a]Determined by MTT assay; T/C% values after 7 days of incubation with anti-BSP IgY. [b]T/C% values of colony counts at day 7 after plating; for treatment the cells were pre-incubated with anti-BSP IgY for 2 days. [c]Number of migrating cells in % of untreated control; T/C% values at day 1 after pre-incubation of MDA-MB-231^{GFP} cells with anti-BSP IgY. [d]Mean growth rate (per day): mean of growth rates (day 1/day 2 and day 2/day 3) determined in cells migrating through pores with a diameter of 8 μm; MGR of control: 0.80.

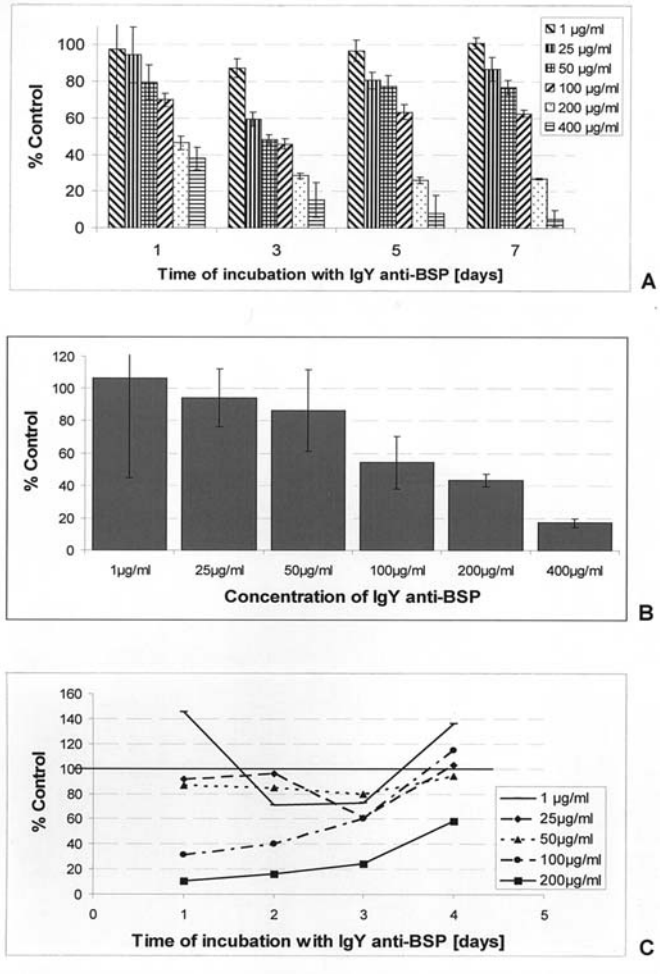

Figure 1. Results of *in vitro* experiments. Proliferation (A), colony formation (B) and migration (C) of MDA-MB-231^{GFP} human breast cancer cells after incubation with an IgY antibody against bone sialoprotein. Values are given as percent of control versus time of incubation. Error bars: standard deviation.

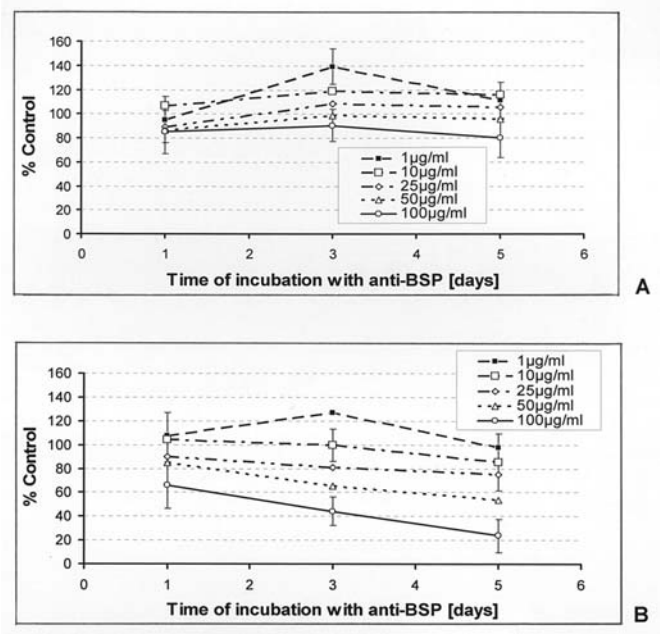

Figure 2. Proliferation of MDA-MB-231^{GFP} cells determined by MTT assay after incubation with a non-specific IgY antibody (A) or with the anti-BSP IgY (B). Values are given as percent of control versus time of incubation. Error bars: standard deviation.

Migration assay. In a transwell migration model, MDA-MB-231^{GFP} cells were exposed in medium containing 1-200 μg/ml anti-BSP in order to examine the inhibition of their migration through pores of 8 μm diameter towards osteoblast-like SAOS-2 cells (Fig. 1C). Following pre-incubation for 2 days, MDA-MB-231^{GFP} cells showed enhanced migration in response to 1 μg/ml anti-BSP (146 T/C%, day 1). Cells pre-incubated with higher concentrations of anti-BSP (25-200 μg/ml) showed decreased T/C% values ranging from 92 to 11 (25-200 μg/ml, day 1). This inhibition of migration decreased gradually with time. At day 4 after exposure, only cells pre-incubated with 200 μg/ml anti-BSP showed significantly reduced migration (59 T/C%) compared to untreated control cells. Cells that had migrated towards the bottom layer were allowed to proliferate for up to three days. Their mean growth rates (MGR; Table I) ranged from 0.64 (25 μg/ml) to 0.25 (200 μg/ml), as compared to the MGR of untreated controls (0.80).

Anti-BSP IgY vs. a non-specific IgY antibody. In a proliferation assay, the effect of another batch of specific IgY antibody against BSP was compared with the effect of a non-specific IgY antibody (Fig. 2). MDA-MB-231^{GFP} cells were incubated for up to 5 days at concentrations from 1 to 100 μg/ml. Exposure to the non-specific IgY was correlated with T/C%

Table II. Design of *in vivo* experiments.

Group no.	Animal no. (% total study)	Mode of treatment	Agent	Concentration/ dosage	Time period of exposure/ treatment schedule
1	25 (30.9)[a]	Untreated control rats	-	-	-
2	9 (11.1)	Pre-treatment of cells (HD[b])	Anti-BSP IgY	600 μg/ml	2 h[f]
3	11 (13.6)	Pre-treatment of cells (LD[c])	Anti-BSP IgY	25-100 μg/ml	48 h[f]
4	12 (14.8)	Early treatment	Anti-BSP IgY	20 mg/kg s.c.	Day 0, 2, 4[g]
5	8 (9.9)	Late treatment (APC[d])	$ErPC_3$	60 μmol/kg i.v.	Twice weekly for 8 weeks[h]
6	8 (9.9)	Late treatment (AB[e])	Anti-BSP IgY	10 mg/kg s.c.	Once weekly for 8 weeks[h]
7	8 (9.9)	Late treatment (APC + AB)	$ErPC_3$ + anti-BSP IgY	60 μmol/kg i.v. $ErCP_3$ + 10 mg/kg s.c. anti-BSP	Twice weekly ($ErPC_3$) plus once weekly (anti-BSP) for 8 weeks[h]

[a]Two rats with spontaneous regression were excluded; the initial number was 27. [b]High dose. [c]Low dose. [d]Alkylphosphocholine. [e]Antibody. [f]Pre-incubation of MDA-MB-231^{GFP} cells before tumor implantation. [g]Three injections of 20 mg/kg were given subcutaneously on days 0, 2 and 4 after tumor implantation. [h]Treatment of rats after the occurrence of lytic lesions.

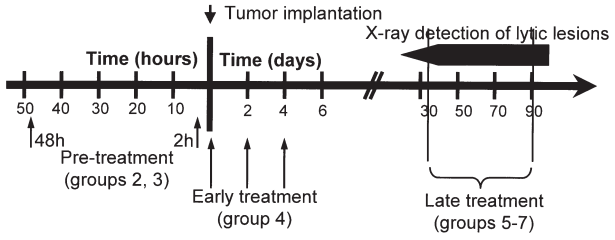

Figure 3. Time axis of *in vivo* experiment. *In vivo* experiments were performed with pre-treated MDA-MB-231^{GFP} cells, which were incubated with anti-BSP IgY for 2 days (group 3) or 2 h (group 2) before implantation into nude rats (pre-treatment). Animals of group 4 received the anti-BSP IgY at the day of tumor implantation, as well as 2 and 4 days later (early treatment). In groups 5-7, treatment was administered to rats with lytic lesions for 8 weeks (late treatment).

values ranging from 116 (10 μg/ml) to 80 (100 μg/ml) at day 5 of the experiment (Fig. 2A). Treatment with the specific anti-BSP IgY resulted in a dose-dependent decrease of cell proliferation ranging from 98 (1 μg/ml) to 24 (100 μg/ml; Fig. 2B) T/C% after 5 days of incubation.

In vivo study. Lytic skeletal lesions were induced by intra-arterial injection of 1x10^5 MDA-MB-231^{GFP} cells into the superficial epigastric artery of nude rats. Subsequent bone metastasis occurred exclusively in the femur, tibia and fibula of the respective hind leg after 3-4 weeks following tumor cell implantation. Number and size of lytic lesions were followed up by X-rays (Fig. 4) and computed tomography (Fig. 6).

The whole *in vivo* study comprised of seven groups of nude rats with a total number of 81 animals (Table II). Untreated control rats (group 1, n=25) were observed for a period of 90 days. The effect of the antibody was assessed by either exposing MDA-MB-231^{GFP} cells prior to their implantation (groups 2 and 3) or by treating rats bearing

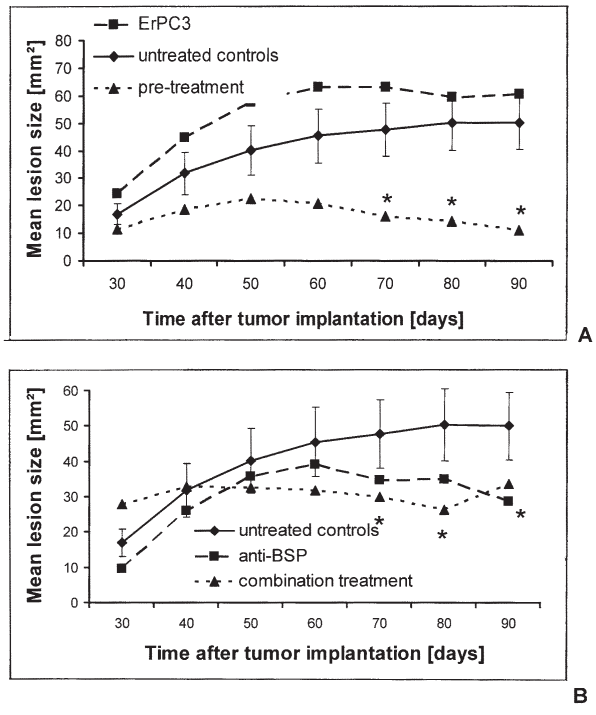

Figure 4. Results of *in vivo* experiments. Comparison of the mean lytic lesion sizes of untreated control rats and animals receiving pre-treatment for 48 h (A), late treatment with $ErPC_3$ (A) or the anti-BSP IgY ± $ErPC_3$ (B). Error bars: standard error. Asterisks denote a significant difference versus control rats ($p<0.05$).

MDA-MB-231^{GFP} cells early (group 4) or late (groups 5-7) after tumor inoculation (Fig. 3). Early treatment started at the day of tumor inoculation and additional s.c. injections were given 2 and 4 days later. Late treatment was administered to rats after the appearance of lytic lesions (Fig. 3). Treatment with the alkylphosphocholine $ErPC_3$, used as control, was given i.v. after the onset of lytic lesions (31-34 days following

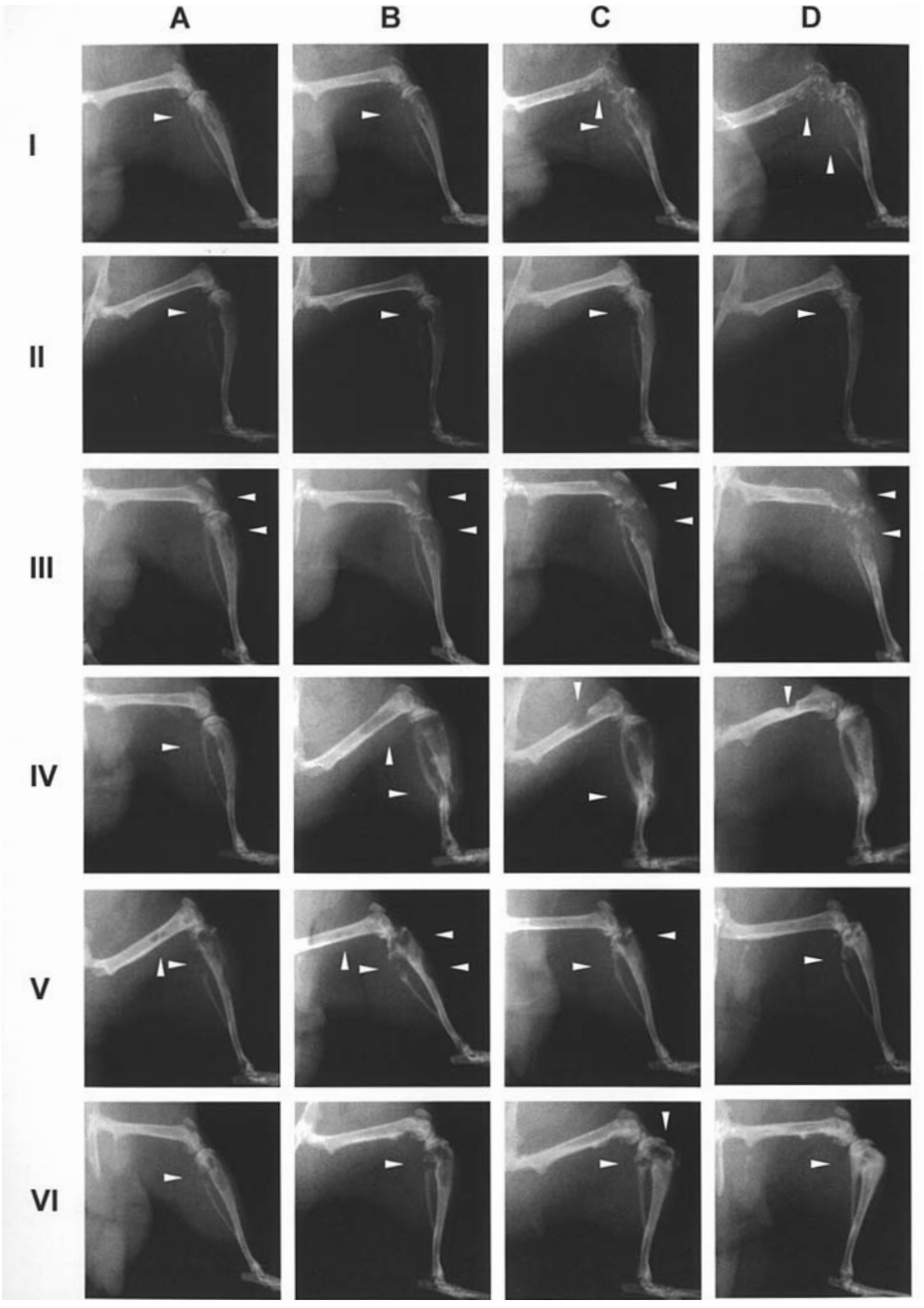

Figure 5. Radiographic comparison of lytic lesions in the right hind leg of nude rats (lesions are indicated by arrows). Serial X-rays of experimental rats taken after 30-35 days (A), 40-45 days (B), 60-65 days (C) and 80-95 days (D) after tumor cell implantation. Roman numbers denote individual animals which are typical for the whole group. These include an untreated control rat (I, group 1), a rat (II) receiving pre-treated MDA-MB-231^{GFP} cells (group 3), a rat (III) treated with $ErPC_3$ (group 5), two rats (IV and V) treated with anti-BSP IgY antibody, and a rat (VI) treated with $ErPC_3$ plus the IgY antibody (group7).

tumor inoculation; group 5, Table II) for a period of 8 weeks. Treatment with anti-BSP IgY and the combination consisting of $ErPC_3$ and anti-BSP was maintained over the same time period (groups 6 and 7, Table II). The antibody and $ErPC_3$ was tolerated well without any side effects.

Pre-treatment. The mean lytic lesion size of animals implanted with MDA-MB-231^{GFP} cells increased more slowly and was significantly smaller at days 70-90 than the corresponding mean lesion size of untreated controls (Fig. 4A). One of 11 rats (9%) did not develop any visible metastasis during the observation time of 90 days.

A representative animal is shown in Fig. 5, lane II and is compared with a control rat (Fig. 5, lane I). The lesion size increased until day 40 (Fig. 5A and B, lane II) and decreased thereafter (Fig. 5C and D, lane II), whereas that of the control animal increased continuously.

Rats receiving pre-treated cells (groups 2 and 3) showed no circular defects of cortical bone or any soft tissue metastasis surrounding the lytic lesions during the observation time of up to 90 days (Table III). Untreated control rats developed a circular defect of cortical bone in 9 of 25 rats (36%) and soft tissue metastasis in 8 of 25 cases (32%; Table III). In comparison to untreated control

Table III. Results of *in vivo* experiments.

Parameter observed	Group 1	Group 2	Group 3	Group 4	Group 5	Group 6	Group 7
T/C%[a] (day 30)	100	37.6[b]	67.2[b]	48.6[b]	143.1	56.1	164.1
T/C%[a] (day 60)	100	18.7[b,f]	45.7[b]	29.9[b,f]	138.7	86.1	70.3
T/C%[a] (day 80)	100	[c]	28.8[b,f]	[c]	118.6	69.5	52.5[f]
T/C%[a] (day 90)	100	[c]	22.4[b,f]	[c]	121.2	57.3[f]	67.5
Rats with circular defects of cortical bone (%)[d]	9 (36)	0 (0)[f]	0 (0)[f]	0 (0)[f]	3 (37.5)	2 (25)	2 (25)
Rats with soft tissue metastasis (%)	8 (32)	0 (0)[f]	0 (0)[f]	0 (0)[f]	3 (37.5)	2 (25)	1 (12.5)
No. of rats without visible metastasis (%)/ no. of complete remissions (%)	- 2 (7.4)	1 (11.1) -	1 (9.1) -	2 (20) -	- 2 (25)	- 1 (12.5)	- 0 (0)
Average daily growth rate of lytic lesions[e] (day 30-90) (mm^2)	0.55	0.07[f]	-0.01[f]	0.18[f]	0.61	0.32[f]	0.10[f]

[a]Mean lytic lesion size of experimental rats in percent of the corresponding lesion size of untreated controls. [b]Mean value excluding rats without any visible metastasis. [c]Group terminated at day 60 after tumor implantation. [d]Circular defects of femur or tibia potentially resulting in a bone fracture; circular defects of the fibula were excluded. [e]Average daily growth rate from day 30 to 90 after tumor implantation for groups 1, 3, 5-7 and from day 30 to 60 for groups 2 and 4. [f]Significant difference versus control rats ($p<0.05$).

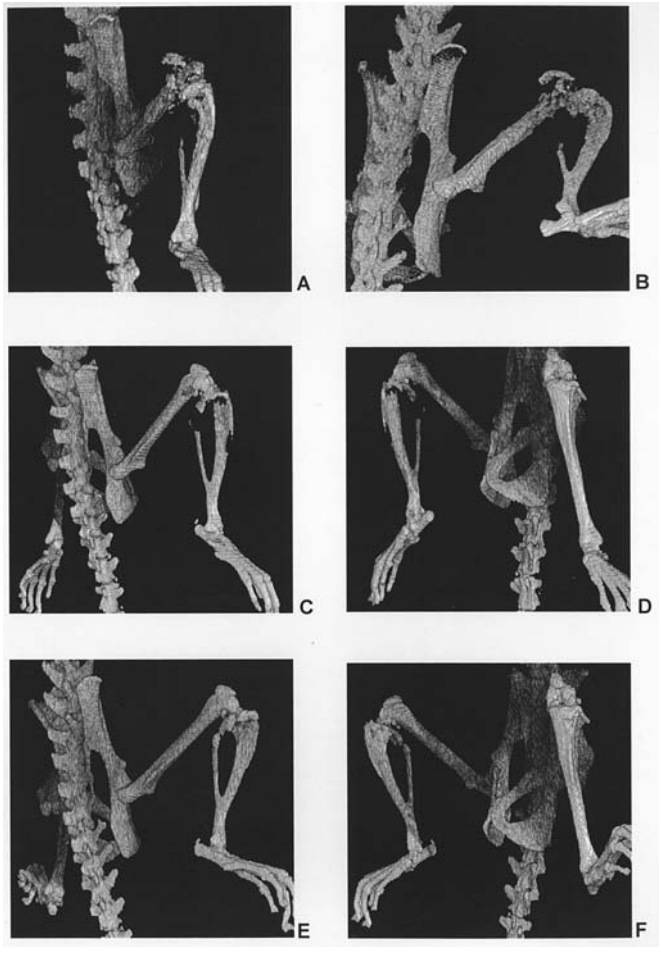

Figure 6. Comparison of computed tomography scan reconstructions of lytic lesions in the right hind leg of nude rats. Computed tomography reconstructions of an untreated control rat also shown in Fig. 5, lane I at day 90 after tumor cell inoculation (A and B) and a rat treated with anti-BSP also shown in Fig. 5, lane V at days 50 (C and D) and 90 (E and F).

rats, the average daily growth rate was distinctly lower in animals receiving pre-treatment. For animals of group 2, the average daily growth rate was 0.07 mm^2 and for those of group 3 it was negative (-0.01 mm^2). In contrast, lesions of untreated control rats increased by 0.55 mm^2 per day on average.

Late treatment. The mean lesion size of animals receiving $ErPC_3$ (group 5, Table II) increased from day 30 (24 mm^2) to day 60 (63 mm^2) after tumor implantation, and then reached a plateau (Fig. 4A). There was no statistically significant difference to untreated control rats during the observation time. A representative lesion treated with $ErPC_3$ is shown in Fig. 5, lane III.

The mean lytic lesion size of animals treated with 10 mg/kg anti-BSP increased from day 30 (10 mm^2) to day 60 (39 mm^2) after tumor implantation (group 6, Table II; Fig. 4B). Thereafter, the average lesion size decreased significantly to a minimum size at day 90 (29 mm^2, $p<0.05$) in comparison to untreated controls. The average daily growth rate was 0.32 mm^2 compared to 0.55 mm^2 for the controls (Table III). Lanes IV and V (Fig. 5) show the course of lytic lesions during the treatment with 10 mg/kg anti-BSP. Overt lytic lesions (Fig. 5A and B, lanes IV and V) were present at days 30-45 after tumor implantation. At days 60-65 (Fig. 5C, lanes IV and V), bone formation was observed in the femur and tibia, especially at the tibial fracture of the animal shown in Fig. 5C, lane IV. On computed tomography reconstructions (Fig. 6) of the same animal as shown in Fig. 5, lane V (Fig. 6C-F), the new bone formation in response to anti-BSP treatment can be seen with greater plasticity. For comparison, the aspect of a lytic lesion is given at the end of the observation period for the same untreated control rat (Fig. 6A and B) as shown in Fig. 5, lane I.

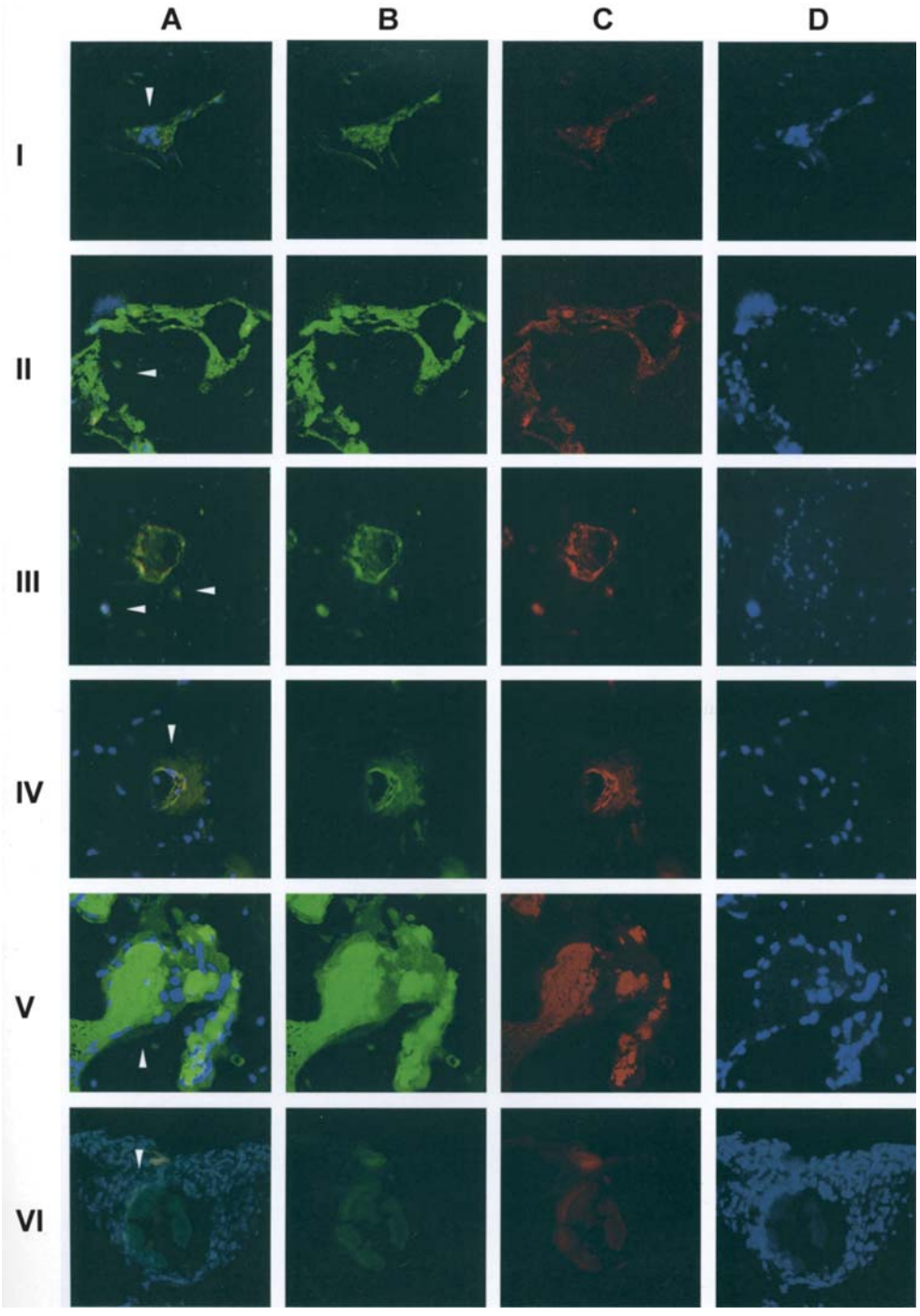

Figure 7. Immunofluorescence labeling of blood vessels within bone (black) as revealed by triple staining (A) of GFP (green), an antibody against human BSP (red, lanes I-V only) and DAPI staining of nuclei (blue). (B-D) Show the respective single color channels for GFP (B, green), human BSP (C, red) and nuclei (D, blue). Lanes I-III: sequential steps following haematogenous spread of MDA-MB-231 cells (arrows) via a small blood vessel (I) such as migration across the endothelial wall (II) and invasion into surrounding bone (III); arrows: MDA-MB-231 cells. Lane IV: oblique cut through a vessel (arrow) staining positive for GFP (B) and human BSP (C). Lane V: cell detritus of MDA-MB-231 cells staining positive for GFP (B) and human BSP (C) after blood vessel embolisation of MDA-MB-231 cells; arrows: cell detritus. Lane VI: MDA-MB-231 cells within a blood vessel; staining with an antibody against anti-BSP IgY (C) shows the presence of anti-BSP IgY on MDA-MB-231 cell surfaces; arrow: anti-BSP on surface of MDA-MB-231 cells.

The average lytic lesion size of animals receiving both, $ErPC_3$ and anti-BSP (group 7, Fig. 4B) increased minimally from 28 mm^2 to 32 mm^2 at day 60 and to 34 mm^2 at day 90 after tumor cell implantation. The average growth per day was 0.1 mm^2 (Table III). At days 70 and 80, the mean lytic lesion size was significantly smaller than that of untreated control animals (30 mm^2 and 26 mm^2, $p<0.05$). Bone lesions in the femur, tibia and fibula of a rat receiving anti-BSP and $ErPC_3$ are shown in Fig. 5, lane VI. Bone formation in the distal femur and the proximal tibia and fibula was observed at days 60-80 (Fig. 5C and D, lane VI).

Animals receiving late treatment with the antibody alone or in combination showed fewer complications such as circular bone lysis or soft tissue metastasis caused by the growth of lytic lesions in comparison to untreated control rats (Table III).

Histology. Rats were sacrificed after a period of 120 days following tumor cell inoculation and histological sections of the right tibia and femur were prepared. These sections were stained with hematoxylin/eosin (HE) and analyzed by immunohistochemistry (Fig. 7).

In preparations stained with HE (data not shown) the tumor cells formed large conglomerations in the bone marrow cavity adjacent to cortical bone, and also clusters within and around osseous blood vessels.

Fig. 7 shows small osseous blood vessels subjected to immunohistochemistry. In lane I, a cluster of MDA-MB-231 cells (A, arrow), which express GFP (B) and BSP (C), is located within a blood vessel. In lane II, a group of breast cancer cells (A, arrow) is to migrate through the endothelium and to leave the blood circulation towards surrounding bone. Single disseminated tumor cells within bone (A, lane III, arrows) are visible in the vicinity of an endothelium staining strongly positive for GFP and BSP (lanes III and IV). In some vessels (lane V), cell detritus of MDA-MB-231 cells without nuclei (Fig. 7D) but still positive for GFP and BSP is detected. These residues may have resulted from tumor cell embolisation (lane V, arrows).

In all sections examined, the green fluorescence indicating GFP expressing MDA-MB-231 cells (Fig. 7B) was co-localized with red fluorescence indicating BSP expression (Fig. 7C). This co-localization of GFP and BSP was also detected at the endothelium of blood vessels (Fig. 7C and D, lanes II-V).

When using an antibody against the anti-BSP IgY, the anti-BSP used for treatment was detected at the surface of MDA-MB-231^{GFP} cells located in a blood vessel (red fluorescence; Fig. 7C, lane VI). Remarkably, this co-localization was detected one month after the final anti-BSP IgY administration.

Discussion

Our aim was to develop a targeted treatment of osteolytic lesions in a nude rat model of site-specific breast cancer bone metastasis. For this purpose, we focused on the role of bone sialoprotein (BSP) in osteolytic lesions induced by MDA-MB-231 human breast cancer cells, and studied the effect of treating nude rats with an antibody against BSP.

In experimental models, MDA-MB-231 human breast cancer cells have been shown to express BSP at both, mRNA and protein levels (5,9). The transfection of these cells with BSP cDNA was associated with increased migration and invasion *in vitro* and *in vivo* (25-27). MDA-MB-231 clones overexpressing BSP showed increased invasion into a collagen matrix (26) and promoted tumor cell migration through bone marrow endothelial cells in a matrigel system (27). In line with previous *in vitro* experiments (23), we were able to show that an antibody against bone sialoprotein decreased proliferation, colony formation and migration in MDA-MB-231 human breast cancer cells. The anti-proliferative effect was observed by the specific antibody against BSP only, but not by the unspecific control IgY. The decrease in proliferation and colony formation of MDA-MB-231 cells was clearly concentration-dependent.

Nude rats, which had been inoculated with MDA-MB-231 cells following 2 days of incubation with the anti-BSP antibody, showed significantly reduced bone metastasis formation compared to rats inoculated with untreated cells. In addition, prolonged treatment of overt osteolytic lesions with the anti-BSP antibody resulted in a partial regression of these lesions as well as in new bone formation and re-mineralization of the affected skeletal structures. These results are in agreement and extend those of an *in vivo* model, in which antibodies against BSP were able to prevent the migration of MDA-MB-231 cells transfected with BSP cDNA (27). Also, van der Pluijm *et al* have shown that the adhesion of MDA-MB-231 cells to extracellular bone matrix could be inhibited by the application of BSP peptides (28).

The suitability of the anti-BSP antibody for a combination therapy was tested by co-administering the antibody with the alkylphosphocholine $ErPC_3$. This agent has been shown to reduce proliferation, colony formation and migration in MDA-MB-231 cells *in vitro* (23). It is also known to be effective against primary rat carcinomas induced by methylnitrosourea (29). In nude rats with bone metastasis, this drug alone caused no reduction in lytic lesion size, but the combination with anti-BSP resulted in a significant decrease in mean osteolytic lesion size. Also, new bone formation was observed in rats treated with anti-BSP + $ErPC_3$. This *de novo* bone formation resulted in almost complete remissions of lytic lesions as well as in stabilization of pathologically fractured bones in some rats.

In the pathogenesis of bone metastasis, primary tumor cells are thought to form aggregates in distant capillaries, to adhere to vascular endothelial cells and to migrate towards the bone marrow stroma by extravasation. For establishing lytic lesions, they have to reach the endosteal bone surface and then are able to modulate the activity of osteoclasts and osteoblasts (30).

In our study, immunohistochemistry revealed further aspects concerning the role of BSP in the pathogenesis of bone metastasis. We were able to visualize processes such as aggregate formation of tumor cells in blood vessels, migration of these cells across the endothelial wall and invasion of MDA-MB-231 cells into surrounding bone. On all sections, the green fluorescence of GFP was co-localized with the red fluorescence of BSP. Especially the endothelium of blood vessels stained strongly for both, GFP and BSP, which indicates that BSP is involved in adhesion of tumor cells to the vessel wall as well in migration of MDA-MB-231 cells through the endothelium.

The anti-BSP IgY was detected on the surface of MDA-MB-231 cells even one month after its final s.c. application by a specific antibody, which indicates a long half-life of this therapeutical antibody.

Two binding partners of BSP, the matrix metalloproteinase MMP-2 and the integrin α(v)ß3, were also assumed to play a critical role in breast cancer concerning tumor cell adhesion, progression and invasion (31-34). In breast cancer patients, these proteins were associated with adverse prognosis (35-37). Many interactions between BSP, MMP-2 and α(v)ß3 have been described (38-41). On the surface of invasive cells as well as on angiogenic blood vessels, α(v)ß3 was observed to form complexes with MMP-2, which increased the invasive potential of these cells (42). Recently, Karadag *et al* described cells using BSP as bridge to link MMP-2 to its

cell surface receptor α(v)ß3 (20). The formation of this trimolecular complex was stimulated by BSP and increased the invasiveness of cancer cells (20). We suggest that inhibiting this complex of BSP, MMP-2 and α(v)ß3 by the anti-BSP antibody has the potential to reduce tumor cell adhesion, migration and invasion in breast cancer bone metastasis.

In untreated control rats, circulating MDA-MB-231 cells were observed for up to 120 days after tumor cell inoculation (21). Upon treatment with anti-BSP, MDA-MB-231 cells circulating within osseous vessels were prevented to extravasate towards the surrounding bone matrix. Consequently, reduced osteolytic lesion sizes were observed in rats that had been treated with the antibody against BSP before or after the appearance of skeletal metastasis. Remarkably, formation of new bone has previously not been described after treating overt osteolytic lesions. Even bisphosphonates being the most widely used treatment for patients with breast cancer bone metastasis are only able to delay the growth and progression of skeletal lesions by inhibiting osteoclast-mediated bone resorption (43-45).

In conclusion, the IgY antibody against BSP has potential for treating breast cancer bone metastasis in a nude rat model, and this type of treatment might be used for preventive or adjuvant purposes in breast cancer patients.

Acknowledgements

We thank Professor B. Krempien for valuable discussions and Ms. B. Kahn for excellent technical guidance.

References

1. Guise TA: Molecular mechanisms of osteolytic bone metastases. Cancer 88 (Suppl 12): 2892-2898, 2000.
2. Coleman RE: Skeletal complications of malignancy. Cancer 80 (Suppl 8): 1588-1594, 1997.
3. Clohisy DR and Mantyh PW: Bone cancer pain. Cancer 97 (Suppl 3): 866-873, 2003.
4. Withold W, Armbruster FP, Karmatschek M and Reinauer H: Bone sialoprotein in serum of patients with malignant bone diseases. Clin Chem 43: 85-91, 1997.
5. Bellahcene A, Antoine N, Clausse N, Tagliabue E, Fisher LW, Kerr JM, Jares P and Castronovo V: Detection of bone sialoprotein in human breast cancer tissue and cell lines at both protein and messenger ribonucleic acid levels. Lab Invest 75: 203-210, 1996.
6. Diel IJ, Solomayer EF, Seibel MJ, Pfeilschifter J, Maisenbacher H, Gollan C, Pechterstorfer M, Conradi R, Kehr G, Boehm E, Armbruster FP and Bastert G: Serum bone sialoprotein in patients with primary breast cancer is a prognostic marker for subsequent bone metastasis. Clin Cancer Res 5: 3914-3919, 1999.
7. Fedarko NS, Jain A, Karadag A, van Eman MR and Fisher LW: Elevated serum bone sialoprotein and osteopontin in colon, breast, prostate, and lung cancer. Clin Cancer Res 7: 4060-4066, 2001.
8. Bellahcene A, Menard S, Bufalino R, Moreau L and Castronovo V: Expression of bone sialoprotein in primary human breast cancer is associated with poor survival. Int J Cancer 69: 350-353, 1996.
9. Ibrahim T, Leong I, Sanchez-Sweatman O, Khokha R, Sodek J, Tenenbaum HC, Ganss B and Cheifetz S: Expression of bone sialoprotein and osteopontin in breast cancer bone metastases. Clin Exp Metastasis 18: 253-260, 2000.
10. Waltregny D, Bellahcene A, De Leval X, Florkin B, Weidle U and Castronovo V: Increased expression of bone sialoprotein in bone metastases compared with visceral metastases in human breast and prostate cancers. J Bone Miner Res 15: 834-843, 2000.
11. Carlinfante G, Vassiliou D, Svensson O, Wendel M, Heinegard D and Andersson G: Differential expression of osteopontin and bone sialoprotein in bone metastasis of breast and prostate carcinoma. Clin Exp Metastasis 20: 437-444, 2003.
12. Fisher LW, Torchia DA, Fohr B, Young MF and Fedarko NS: Flexible structures of SIBLING proteins, bone sialoprotein, and osteopontin. Biochem Biophys Res Commun 280: 460-465, 2001.
13. Fisher LW, Jain A, Tayback M and Fedarko NS: Small integrin binding ligand N-linked glycoprotein gene family expression in different cancers. Clin Cancer Res 10: 8501-8511, 2004.
14. Ganss B, Kim RH and Sodek J: Bone sialoprotein. Crit Rev Oral Biol Med 10: 79-98, 1999.
15. Fisher LW, Whitson SW, Avioli LV and Termine JD: Matrix sialoprotein of developing bone. J Biol Chem 258: 12723-12727, 1983.
16. Bianco P, Fisher LW, Young MF, Termine JD and Robey PG: Expression of bone sialoprotein (BSP) in developing human tissues. Calcif Tissue Int 49: 421-426, 1991.
17. Tye CE, Hunter GK and Goldberg HA: Identification of the type I collagen-binding domain of bone sialoprotein and the mechanism of interaction. J Biol Chem 280: 13487-13492, 2005.
18. Ross FP, Chappel J, Alvarez JI, Sander D, Butler WT, Farach-Carson MC, Mintz KA, Robey PG, Teitelbaum SL and Cheresh DA: Interactions between the bone matrix proteins osteopontin and bone sialoprotein and the osteoclast integrin alpha v beta 3 potentiate bone resorption. J Biol Chem 268: 9901-9907, 1993.
19. Somerman MJ, Fisher LW, Foster RA and Sauk JJ: Human bone sialoprotein I and II enhance fibroblast attachment *in vitro*. Calcif Tissue Int 43: 50-53, 1988.
20. Karadag A, Ogbureke KU, Fedarko NS and Fisher LW: Bone sialoprotein, matrix metalloproteinase 2, and alpha(v)beta3 integrin in osteotropic cancer cell invasion. J Natl Cancer Inst 96: 956-965, 2004.
21. Bäuerle T, Adwan H, Kiessling F, Hilbig H, Armbruster FP and Berger MR: Characterization of a rat model with site-specific bone metastasis induced by MDA-MB-231 breast cancer cells and its application to the effects of an antibody against bone sialoprotein. Int J Cancer 115: 177-186, 2005.
22. Adwan H, Bäuerle TJ and Berger MR: Downregulation of osteopontin and bone sialoprotein II is related to reduced colony formation and metastasis formation of MDA-MB-231 human breast cancer cells. Cancer Gene Ther 11: 109-120, 2004.
23. Adwan H, Bäuerle T, Najajreh Y, Elazer V, Golomb G and Berger MR: Decreased levels of osteopontin and bone sialoprotein II are correlated with reduced proliferation, colony formation, and migration of GFP-MDA-MB-231 cells. Int J Oncol 24: 1235-1244, 2004.
24. Ganten D and Ruckpaul K: Molekular- und Zellbiologische Grundlagen. Springer Verlag, Berlin, Heidelberg, 1997.
25. Zhang JH, Tang J, Wang J, Ma W, Zheng W, Yoneda T and Chen J: Over-expression of bone sialoprotein enhances bone metastasis of human breast cancer cells in a mouse model. Int J Oncol 23: 1043-1048, 2003.
26. Sharp JA, Waltham M, Williams ED, Henderson MA and Thompson EW: Transfection of MDA-MB-231 human breast carcinoma cells with bone sialoprotein (BSP) stimulates migration and invasion *in vitro* and growth of primary and secondary tumors in nude mice. Clin Exp Metastasis 21: 19-29, 2004.
27. Chen J, Rodriguez JA, Barnett B, Hashimoto N, Tang J and Yoneda T: Bone sialoprotein promotes tumor cell migration in both *in vitro* and *in vivo* models. Connect Tissue Res 44 (Suppl 1): 279-284, 2003.
28. Van der Pluijm G, Vloedgraven HJ, Ivanov B, Robey FA, Grzesik WJ, Robey PG, Papapoulos SE and Lowik CW: Bone sialoprotein peptides are potent inhibitors of breast cancer cell adhesion to bone. Cancer Res 56: 1948-1955, 1996.
29. Berger MR, Sobottka S, Konstantinov SM and Eibl H: Erucylphosphocholine is the prototype of i.v. injectable alkylphosphocholines. Drugs Today 34 (Suppl F): 73-81, 1998.
30. Mundy GR: Metastasis to bone: causes, consequences and therapeutic opportunities. Nat Rev Cancer 2: 584-593, 2002.
31. Egeblad M and Werb Z: New functions for the matrix metalloproteinases in cancer progression. Nat Rev Cancer 2: 161-174, 2002.
32. Tester AM, Waltham M, Oh SJ, Bae SN, Bills MM, Walker EC, Kern FG, Stetler-Stevenson WG, Lippman ME and Thompson EW: Pro-matrix metalloproteinase-2 transfection increases orthotopic primary growth and experimental metastasis of MDA-MB-231 human breast cancer cells in nude mice. Cancer Res 64: 652-658, 2004.
33. Hood JD and Cheresh DA: Role of integrins in cell invasion and migration. Nat Rev Cancer 2: 91-100, 2002.

34. Pecheur I, Peyruchaud O, Serre CM, Guglielmi J, Voland C, Bourre F, Margue C, Cohen-Solal M, Buffet A, Kieffer N and Clezardin P: Integrin alpha(v)beta3 expression confers on tumor cells a greater propensity to metastasize to bone. FASEB J 16: 1266-1268, 2002.
35. Leppa S, Saarto T, Vehmanen L, Blomqvist C and Elomaa I: A high serum matrix metalloproteinase-2 level is associated with an adverse prognosis in node-positive breast carcinoma. Clin Cancer Res 10: 1057-1063, 2004.
36. Li HC, Cao DC, Liu Y, Hou YF, Wu J, Lu JS, Di GH, Liu G, Li FM, Ou ZL, Jie C, Shen ZZ and Shao ZM: Prognostic value of matrix metalloproteinases (MMP-2 and MMP-9) in patients with lymph node-negative breast carcinoma. Breast Cancer Res Treat 88: 75-85, 2004.
37. Gasparini G, Brooks PC, Biganzoli E, Vermeulen PB, Bonoldi E, Dirix LY, Ranieri G, Miceli R and Cheresh DA: Vascular integrin alpha(v)beta3: a new prognostic indicator in breast cancer. Clin Cancer Res 4: 2625-2634, 1998.
38. Fedarko NS, Jain A, Karadag A and Fisher LW: Three small integrin binding ligand N-linked glycoproteins (SIBLINGs) bind and activate specific matrix metalloproteinases. FASEB J 18: 734-736, 2004.
39. Teti A, Farina AR, Villanova I, Tiberio A, Tacconelli A, Sciortino G, Chambers AF, Gulino A and MacKay AR: Activation of MMP-2 by human GCT23 giant cell tumour cells induced by osteopontin, bone sialoprotein and GRGDSP peptides is RGD and cell shape change dependent. Int J Cancer 77: 82-93, 1998.
40. Byzova TV, Kim W, Midura RJ and Plow EF: Activation of integrin alpha(V)beta(3) regulates cell adhesion and migration to bone sialoprotein. Exp Cell Res 254: 299-308, 2000.
41. Sung V, Stubbs JT III, Fisher L, Aaron AD and Thompson EW: Bone sialoprotein supports breast cancer cell adhesion proliferation and migration through differential usage of the alpha(v)beta3 and alpha(v)beta5 integrins. J Cell Physiol 176: 482-494, 1998.
42. Brooks PC, Stromblad S, Sanders LC, von Schalscha TL, Aimes RT, Stetler-Stevenson WG, Quigley JP and Cheresh DA: Localization of matrix metalloproteinase MMP-2 to the surface of invasive cells by interaction with integrin alpha v beta 3. Cell 85: 683-693, 1996.
43. Conte P and Coleman R: Bisphosphonates in the treatment of skeletal metastases. Semin Oncol 31 (Suppl 10): 59-63, 2004.
44. Clamp A, Danson S, Nguyen H, Cole D and Clemons M: Assessment of therapeutic response in patients with metastatic bone disease. Lancet Oncol 5: 607-616, 2004.
45. Lipton A: Bisphosphonates and breast carcinoma: present and future. Cancer 88 (Suppl 12): 3033-3037, 2000.